www.czasopisma.pan.pl PAN POLSKA AKADEMIA NAUK www.journals.pan.pl

Arch. Metall. Mater. **66** (2021), 3, 911-915

DOI: 10.24425/amm.2021.136397

R. JAGADEESWARI[1], P. SELVAKUMAR[2*], V. JEEVANANTHAM[2], R. SARAVANAN[1]

CHEMICALLY MODIFIED CELLULOSE CAPPED ZINC OXIDE NANOCOMPOSITE: SPECTRAL AND OPTICAL PROPERTIES

In this study, a new chemically modified cellulose polymer-capped ZnO nanopowder prepared by hydrothermal method using chemically modified cellulose polymer as capping agent was successfully reported. The structural characteristics of CMC-capped ZnO nanopowder was reported by FTIR, XRD, SEM and EDX studies. XRD results revealed crystallographic properties like crystal composition, phase purity and crystallite size of the prepared CMC-capped ZnO nanopowder and average size calculated by Debye Scherrer formula as 14.66 nm. EDX studies revealed that the presence of elemental compositions of capping agent in the nanopowder samples. The optical characterization of the CMC-capped ZnO nanopowder was studied using UV absorption (λ_{max} = 303 nm) and PL spectroscopy (λ_{ex} = 295 nm). The average crystal diameter and grain size were calculated by effective mass approximation formula and compared with XRD findings that agreed well and verified CMC capped ZnO with particle size of 193 nm. Thus, the promising optical characteristics shown by the synthesized CMC capped ZnO nanopowders exposes its potential usage in bio-medical fields.

Keywords: Chemically modified cellulose, Hydrothermal, XRD, Surface morphology, effective mass approximation

1. Introduction

Nanomaterials fascinates immense interest due to their extraordinary applications such as sorbents, sensors, ceramic materials, photo-devices, solar cells and as catalysts [1]. Hazardous dye removal from waste water using nanomaterials gained considerable interest mainly due to adsorption properties possessed by these materials such as larger surface area, extraordinary catalytic activity and chemical stability. Metal-organic composites advanced as an efficient material in the adsorption process and numerous materials were fabricated earlier for the application of dye removal which includes fly ash, sand, excluded tea wastes, plant wastes, but the study of organic polymers is limited [2]. Polymer nanocomposite not only applicable to degradation and dye removal studies but also applied to various applications such as conducting devices and anticorrosion properties. The functional groups include a chemical content that imparts the molecule with a hydrophilic character due to hetero atoms associated with functional groups. If the hydrophilic aspect of the capping agent is fully established, so it is dissolvable in the solvent environment and nanomaterial preparation becomes simpler.

In contrast, it should also have a prevailing hydrophobic character (i.e. Presence of alkyl groups) to hold on to nanomaterial nuclei during formation. The above characters available in a chemical substance will serve as suitable capping agents for nanomaterial synthesis [3]. Nanomaterial quantity is high when hetero functionalities found in capping agents imparts ionicity in the molecule and also large enough to stay in the solvent medium. These facts clearly state that hydrophilic character should be minimal and hydrophobicity should be the primary character as nanomaterials nucleate and begin to expand. As the capping agents hook on nanoparticles preferably metal nanoparticles, the charge regulation on metal particles switches to capping agents if they exceed their solubility limit until it builds up to certain sizes. Thus, the capping agents can monitor the shape and size of nanomaterial, which includes the research design an impression of endorsing their work although there is little need to suggest any coherent literature evidence [4]. Therefore, the present researchers are still looking for appropriate capping for their work analysis and the same can be seen over the last twenty years.

There is a 3.37 eV direct band difference and 60 meV of exciton binding energy in zinc. The interfacial linkages should

[1] DEPARTMENT OF CHEMISTRY, KPR INSTITUTE OF ENGINEERING AND TECHNOLOGY, COIMBATORE-641407, TAMILNADU, INDIA
[2] DEPARTMENT OF CHEMISTRY, VIVEKANANDHA COLLEGE OF ARTS AND SCIENCES FOR WOMEN, TIRUCHENGODE-637205, TAMILNADU, INDIA
* Corresponding author: selvakumarpr@gmail.com

be very good in order to obtain great composites. This can be achieved by using a polymer/metal hybrid photocatalyst that will have greater conductivity due to certain heavy metal ions such as ZnO. Encapsulation of conductive-metal nanoparticles that prevents dissolution of conductive ZnO/CMCnanopowders. Hetero-atoms of polymeric carbon cores of different functional groups possess ologies, tunable excitation/emission, nontoxicity, and biodegradability, and ecological friendliness. Its high index of refraction means it may be useful in the fields of bioimaging, photovoltaic chemistry, photochemical, and other fields.

Chemically Modified Cellulose (CMC) have been proven to be a very promising material in producing thermally and electrically conductive polymer nanocomposites but researches are limited [5]. Alteration of cellulose by graft copolymerization and specific chemical modification techniques facilitates a chemical shift of the cellulose chain by adding functional groups, leading to modern cellulose products with new properties [6]. The novel bio-nanocomposite material of Cellulose/copper nanoparticles (CuNP) bio-nanocomposites were prepared using a bio-flocculant as a reductant of the precursor copper ions for the in-situ generation of CuNP in the cellulose matrix useful for diagnostic and biomedical applications [7]. Carboxymethyl cellulose (CMC) capped Ag-ZnO nanoparticles (NPs) were synthesized by chemical (CD) and mechanical deposition (MD) of Ag NPs on ZnO NPs and investigated antimicrobial activity against planktonic and biofilm growing bacteria [8]. A discussion of the different methods of treatment for the cellulose/ZnO preparation, and the resulting effects on morphology and properties have been reported. In addition, high stability of the cellulose/ZnO when prepared with the precipitation method [9]. In search for new chemically modified polymeric cellulose capped ZnO, a pioneer research was recorded and explored its optical characteristics.

2. Materials and methods

All other analytical grade reagents were bought from Merck, India upon without additional purification. Chemically modified cellulose (CMC) polymer synthesis carried out by following steps cellulose monomer dispersed in deionized water was stirred with 0.04M sodium metaperiodate ($NaIO_4$) solution at room temperature in dark as reported earlier [10]. 4 hrs later, a pale-yellow colour cellulose dialdehyde formed was separated and cleaned using distilled water till solution becomes neutral and dried under vacuum. Then 2-Carbon/3-Carbon of (2 g) dialdehyde groups of cellulose were condensed with p-toluidine (3 g) to produce Schiff base in cellulose chain, the reaction was carried out at 70°C with a catalyst as HCl. After 3 hrs of reaction time reddish brown powder of CMC distillates out was cleaned using hot water and C_2H_5OH filtered, then vacuum dried. So as to synthesise Zinc oxide nanoparticles, standard $ZnSO_4$ (0.1 molar) solutions were diluted in methanol (50 ml) with stirring. To the stirred mixture, NaOH (25 ml of 0.2 M) solution diluted in methanol was added with constant stirring to at a constant pH (8-11) of the reactants and 1% CMC was added to the mixture and dispersed in ultrasonicator. Now, the solutions were moved to stainless-steel autoclaves (teflon lined) and held temperatures at 100-200°C for 6-12 hrs beneath the autogenerated pressure. Then mixture permitted to cool down naturally to laboratory temperature, followed by filtering, washing and drying. Dry precipitates were extracted and ground in an agate mortar and processed for later use in a desiccator [11]. The schematic representation is depicted in Fig. 1.

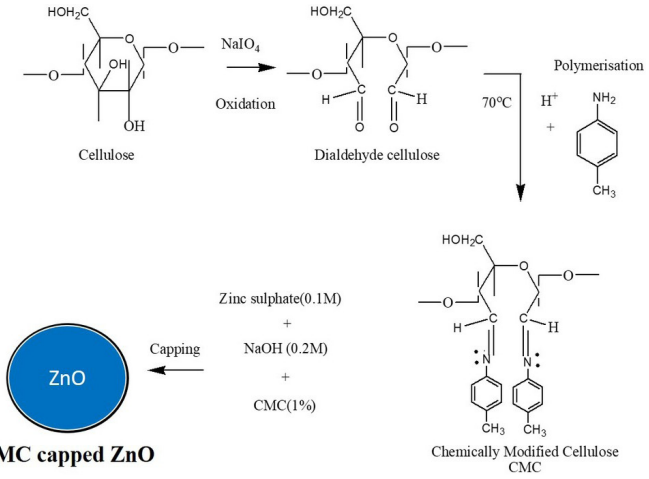

Fig. 1. Schematic illustration of preparation of ZnO/CMC nanocrystallite

The corresponding structural behaviours of crystal-like sample was determined by means of Shimadzu model 6000 X-ray diffraction spectrometer using Cu Kὰ (0.154 nm) as a radiation source to produce sample diffraction patterns at an angle of 2θ of 10-80. Infrared spectroscopy used to study sample bonding (Perkin Elmer-1650 Model). The surface morphology of the nanocomposite was investigated using a FESEM (field Emission scanning electron microscope) with 5 kV acceleration voltage and fitted with EDX (FEI Nova NanoSEM 230). Absorption studies were tested using UV-vis spectrometer (Shimadzu model UV-3600) and photoluminescence (PL) (Perkin Elmer LS 55) were used to analyse the optical properties of materials at room temperatures within a wavelength of 200-800 nm.

3. Results and discussion

3.1. Morphology, crystallinity and elemental studies

FTIR peak at 524.7 cm^{-1} corresponds to the formation of ZnO (Fig. 2). The development of POT-Zn-O exhibited a peak at 3465 cm^{-1} agreeing to the C-H stretching of the CH_3 group. The peak at 1639.76 cm^{-1} agreeing to –N = CH– stretching frequency and the C-N stretching frequency appeared at 1492 cm^{-1} which supports the formation of methyl benzalaniline pendent groups of the chemically modified cellulose. The peak at 1095 cm^{-1} agreeing to C-O-C stretching vibration related to CMC [12].

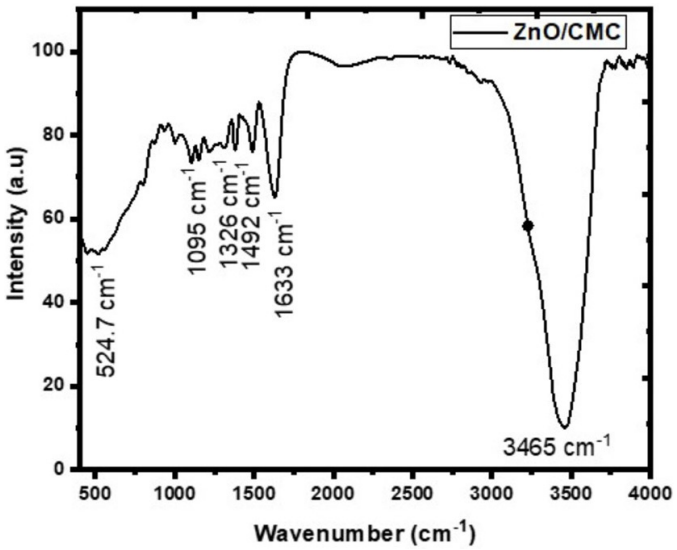

Fig. 2. FTIR spectra of ZnO/CMC nanocrystallite

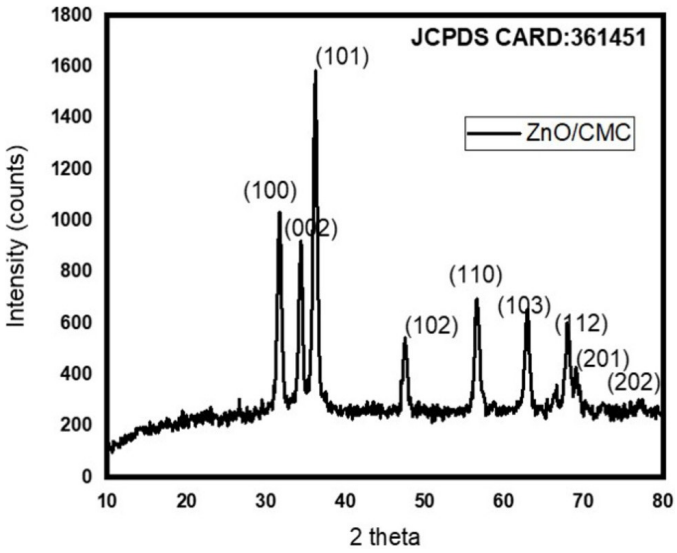

Fig. 3. XRD patterns of ZnO/CMC nanocrystallite

The XRD pattern of ZnO/CMC showed characteristic diffraction peaks (Fig. 3) at 2θ = 26.61°, 33.2°, 34.33°, 37.4°, 47.44°, 56.53°, 62.83°, 66.35°, 67.93°, 69.2°, 72.27° corresponds to 100, 101, 102, 103, 112, 201 and 202 planes of nanocrystalline ZnO. At 2θ = 31.66° and 36.16°, the two peaks correspond to the nanocrystalline ZnO [13]. The findings suggested that within the polymer chain, ZnO/CMC nano-crystallites have been homogeneously mixed with hexagonal structure (JCPDS:361451). Note that the representative peaks of ZnO/CMC are somewhat changed, due to the intense interaction between CMC and ZnO, from their normal location in nanocomposites [14].

The obtained XRD reading from the instrument was deconvoluted using regular Origin 9.0 programme in order to measure the crystallinity using the Debye Scherrer formula Eq. (1).

$$D = k\lambda/(\beta\cos\theta) \qquad (1)$$

Here, k-Scherrer constant (= 0.9), λ – X-ray wavelength, β – peak width of half-maximum and θ – Bragg diffraction angle [15]. By the formula the calculated nanocrystallite size of ZnO/CMC was 14.66 nm for (101) plane.

SEM micrographs studied the surface characteristics of ZnO/CMC and shows this in Fig. 4a. The ZnO/CMC nanocrystaline size observed in the SEM images, was in the range of 193 nm. An inset histogram represented in Fig. 4a. It is apparent from Fig. 4a. that the SEM micrographs display the cubic shape of the synthesized nanopowders of ZnO/CMC [16].

The creation of the hexagonal shape crystal geometry of the ZnO/CMC nanopowders was supported by pre-eminent highly organized growth detected from the SEM images of the satisfactory constituent part. It should have been recalled that the grain nano size of the SEM calculated ZnO/CMC nano powders is similar to the nanoparticle size determined in the X-ray study [17]. The synthesised ZnO/CMC sample size inspected was in nano sized grains, which acts a significant part in improving optical properties of the samples by increasing surface area ratio with thickness [18]. In the meantime, the size decrease in

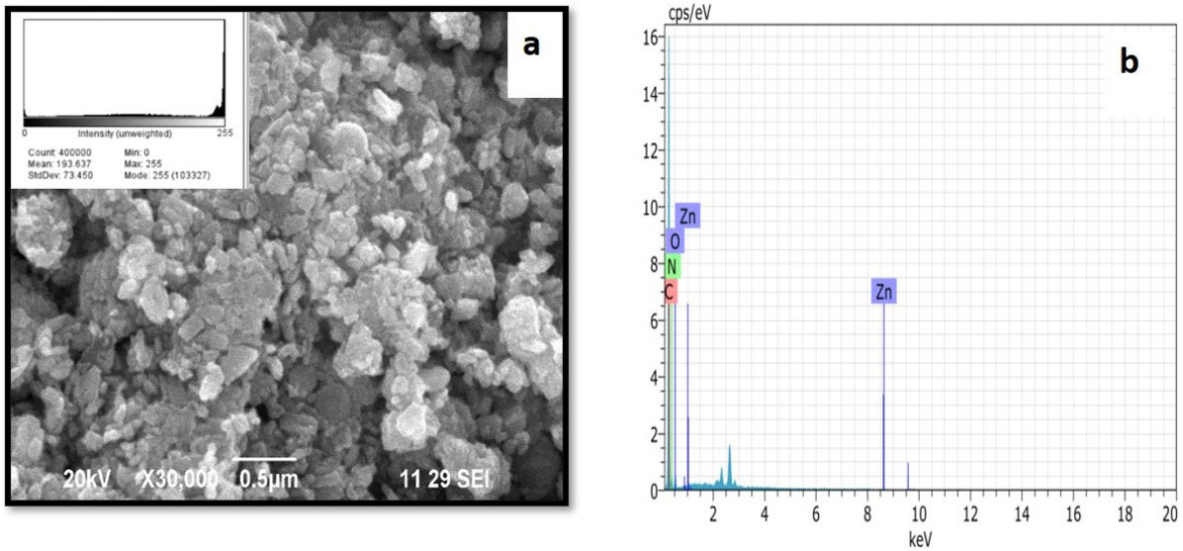

Fig. 4. a) SEM and b) EDS images of ZnO/CMC nanocrystallite

nano-range supports the effect of quantum containment on ZnO/CMC nanopowders, which infers a blueshift due to an increase in band difference.

The carbon, oxygen and nitrogen occurrence of CMC was seen in the EDX spectrum (Fig. 4b) of the capped samples, confirming that capping was successful, as well as the presence of zinc and oxygen, suggesting the formation of CMC-capped ZnO nanopowders [19].

3.2. Optical studies and particle size determination

Fig. 5. displays the absorbance distribution of the synthesised ZnO/CMC nanopowders. From absorbance spectrum (Fig. 5), the ZnO/CMC nanopowders exhibited high absorbance (λ = 250-350 nm) wavelength range with a maximum absorption at 303 nm.

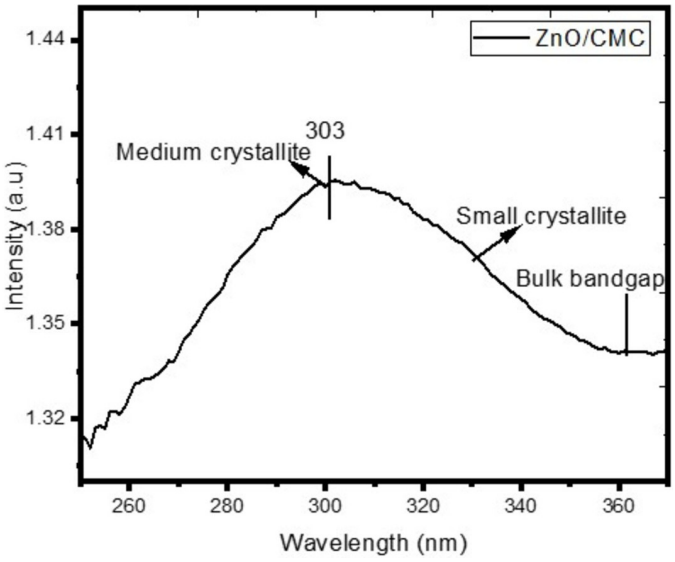

Fig. 5. Ultraviolet absorption spectra of ZnO/CMC nanocrystallite

The absorbance abruptly decreases around 307 nm near the edge of the band, after which it turns to the transmittance field. Blue changes appear in the optical absorption spectra that would mean that the exciton wavelength was approximately 193 nm for the ZnO/CMC nanoparticle, which displayed the most extreme near-edge luminescence, with only mild green luminescence. This study leads us to believe that the green emission is due to the surface traps, e.g., oxygen vacancy. The bulk material is made up of a large number of molecules that form adjacent energy bands. If the particle size approaches the nano size, the number of overlapping energy levels or orbitals reduces, there is an increase in the distance between the valence band and the conduction band. This presents the greater energy difference between bulk-material and nanoparticle states. An electron would not usually pass within a band gap. Electron movement would be more restricted as this forbidden area grows. Also, the absorption spectrum has shifted to the blue-shifted region.

The particle size of ZnO/CMC nanopowders was also measured using the Brus equation Eq. (2). for further confirmation [20].

$$E_{bulk} \cong E_g + \frac{\hbar^2 \Pi^2}{2R^2}\left\{\frac{1}{m_e}+\frac{1}{m_h}\right\} - \frac{1.8e^2}{\in R} \qquad (2)$$

where m_e – effective mass of the electron (0.19), m_h – effective mass of the hole (0.8), R – particle radius, € – dielectric constant (5.7) (selected from size of ZnO/CMC) [21]. At smaller particle diameters, the dielectric constant of the ZnO/CMC nanoparticles decreases. There is usually a slight band gap shift when the size of nanometals is less than the Bohr radius of excitons. However, the ZnO/CMC exciton Bohr radius (around 1.8 nm) is larger than the shift in band gap only represents the confinement effect, suggesting that the band gap effect has been entirely ignored in the design of the nanopowders (diameters above 193 nm). The dielectric constant of ZnO/CMC nanoparticles is found to decrease as the size decreases, which makes them a better conductor [22].

It was observed that the particle radius (size) of ZnO/CMC nanopowders measured by Brus equation ~16.84 nm, which is in close compatible with the size measured by the XRD study of 14.66 nm [23].

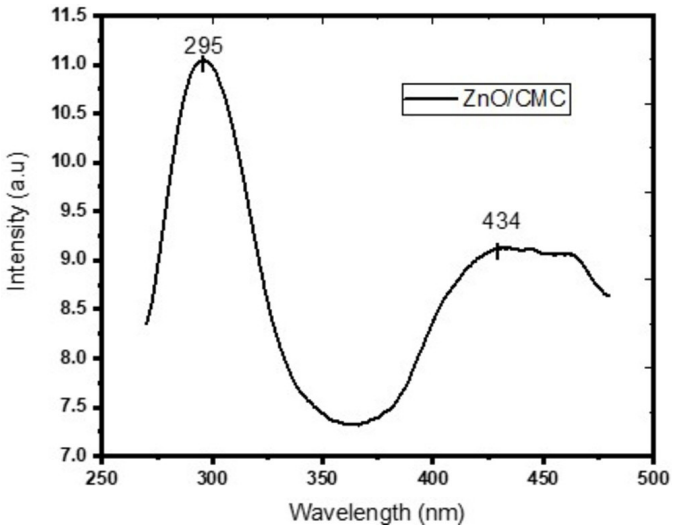

Fig. 6. PL spectra of ZnO/CMC nanocrystallite

Fig. 6. shows the CMC-ZnO at the excitation wavelength of 295 nm, thereby proving the involvement of CMC into ZnO matrix. The significant peak at around 434 nm for nanoparticles synthesized using CMC as capping agent was attributed to the transition from CMC polymer's polaronic band to the π-band (HOMO) structures and the λ_{em} (emission wavelength) was lifted in the direction of blue upon comparing reports of polymer bulk [24]. The electron and hole pairs recombination were attributed to the emission. The strong quantum confinement was demonstrated by the CMC polymer shift towards blue as reported earlier by the researchers. In specific, polymer capping of spectral nanoparticles increased the fluorescence strength due to grain refinement of substrate killer defects [25].

4. Conclusion

A successful report of simple and convenient hydrothermal synthesis of chemically modified cellulose capped ZnO nanoparticle was presented and it is optical properties was elucidated. The nanoparticle confirms the enhancement of well-defined morphological crystallite in polymer capped Zinc oxide nanoparticles. XRD findings affirm nano-crystallographic features of ZnO/CMC. Scanning Electron Microscope often detects surface properties of the prepared ZnO/CMC nanopowders on a nanoscale with hexagonal morphology. The carbon, oxygen and nitrogen occurrence of CMC in the EDX spectrum of the samples, confirming that capping was successful, as well as the presence of zinc and oxygen, suggesting the formation of CMC-capped ZnO nanopowders. The average size of the ZnO/CMC is verified theoretically using effective mass approximation and confirms the presence of nanosized powders with particle size of 16.84 nm which agreed well with XRD findings. The ZnO/CMC nanopowders exhibited high absorbance (λ = 250-350 nm) wavelength range with a maximum absorption at 303 nm. PL studies also revealed involvement of CMC polymer in increasing the fluorescent intensity with an excitation wavelength of 295 nm with blue shift confirms the CMC in ZnO matrix. Above wavelength shift results showed that, ZnO/CMC nanopowders possess optical characteristics and promising contenders for the applications in sensor and medical fields.

Acknowledgement

The authors would like to thank KPR Institute of Engineering & Technology, Coimbatore for extending laboratory facilities towards successful completion of this research work.

Funding

This research did not receive any specific grant from funding agencies in the public, commercial, or not-for-profit sectors.

REFERENCES

[1] M. Abbas, M. Buntinx, W. Deferme, R. Peeters, Nanomaterials **9** (10), 1494 (2019). DOI: https://doi.org/10.3390/nano9101494

[2] J. Chen, Q. Yu, X. Cui, M. Dong, J. Zhang, C. Wang, J. Fan, Y. Zhu, Z. Guo, J. Mater. Chem. C **7** (38), 11710-11730 (2019). DOI: https://doi.org/10.1039/c9tc03655e

[3] S. Huda, M.A. Alam, P.K. Sharma, J. Drug Deliv. Sci. Technol. 102018 (2020). DOI: https://doi.org/10.1016/j.jddst.2020.102018

[4] F. Farjadian, A.R. Akbarizadeh, L. Tayebi, Heliyon **6** (8), e04747 (2020). DOI: https://doi.org/10.1016/j.heliyon.2020.e04747

[5] M.M. Abutalib, A. Rajeh, Polym. Test. 106803 (2020). DOI: https://doi.org/10.1016/j.polymertesting.2020.106803

[6] L. Cen, K.G. Neoh, E T. Kang, Langmuir **19** (24), 10295-10303 (2003). DOI: https://doi.org/10.1021/la035104c

[7] L. Muthulakshmi, A. Varada Rajalu, G.S. Kaliaraj, S. Siengchin, J. Parameswaranpillai, R. Saraswathi, Composites Part B: Engineering, **175**, 107177 (2019). DOI: https://doi.org/10.1016/j.compositesb. 2019.107177

[8] M.V. Lungu, E. Vasile, M. Lucaci, D. Pătroi, N. Mihăilescu, F. Grigore, V. Marinescu, A. Brătulescu, S. Mitrea, A. Sobetkii, A.A. Sobetkii, M. Popa, M.C. Chifiriuc, Materials Characterization **120**, 69-81 (2016). DOI: https://doi.org/10.1016/j.matchar.2016.08.022

[9] Zhao, Si-Wei, Guo, Chong-Rui, Hu, Ying-Zhu, Guo, Yuan-Ru, Pan, Qing-Jiang. Open Chemistry **16** (1), 9-20 (2018). DOI: https://doi.org/10.1515/chem-2018-0006

[10] R. Saravanan, L. Ravikumar, Water Environ. Res. **89** (7), 629-640 (2017). DOI: https://doi.org/10.2175/106143016X14733681696329

[11] J. Wang, S. Yu, H. Zhang, Optik **180**, 20-26 (2019). DOI: https://doi.org/10.1016/j.ijleo.2018.11.062

[12] R. Saravanan, L. Ravikumar, J. Water Resour. Prot. **7** (6), 530 (2015). DOI: https://doi.org/10.4236/jwarp.2015.76042

[13] S. Krishnaswamy, P. Panigrahi, S. Kumaar, G.S. Nagarajan, Nano-Struct. Nano-Objects **22**, 100446 (2020). DOI: https://doi.org/10.1016/j.nanoso.2020.100446

[14] C. Miao, W.Y. Hamad, Curr. Opin. Solid State Mater. Sci. **23** (4), 100761 (2019). DOI: https://doi.org/10.1016/j.cossms.2019.06.005

[15] K.I. Aly, O. Younis, M.H. Mahross, O. Tsutsumi, M.G. Mohamed, M.M. Sayed, Polym. J. **51** (1), 77-90 (2019). DOI: https://doi.org/10.1038/s41428-018-0119-6

[16] K. Rojas, D. Canales, N. Amigo, L. Montoille, A. Cament, L.M. Rivas, O. Gil-Castell, P. Reyes, M.T. Ulloa, A. Ribes-Greus, Compos. Part B Eng. **172**, 173-178 (2019). DOI: https://doi.org/10.1016/j.compositesb.2019.05.054

[17] S. Amjadi, S. Emaminia, S.H. Davudian, S. Pourmohammad, H. Hamishehkar, L. Roufegarinejad, Carbohydr. Polym. **216**, 376-384 (2019). DOI: https://doi.org/10.1016/j.carbpol.2019.03.062

[18] D. Bharathi, R. Ranjithkumar, B. Chandarshekar, V. Bhuvaneshwari, Int. J. Biol. Macromol. **129**, 989-996 (2019). DOI: https://doi.org/10.1016/j.ijbiomac.2019.02.061

[19] K. Rajesh, V. Crasta, N.R. Kumar, G. Shetty, P.D. Rekha, J. Polym. Res. **26** (4), 99 (2019). DOI: https://doi.org/10.1007/s10965-019-1762-0

[20] Y. Yang, W. Guo, X. Wang, Z. Wang, J. Qi, Y. Zhang, Nano letters, **12** (4), 1919-1922 (2012). DOI: https://doi.org/10.1021/nl204353t

[21] Z. R. Khan, M. Arif , A. Singh, International Nano Letters, **2**, 22 (2012). DOI: https://doi.org/10.1186/2228-5326-2-22

[22] F. Rodríguez-Mas, J.C. Ferrer, J.L. Alonso, D. Valiente, S. Fernández de Ávila, Crystals **10** (3), 226 (2020). DOI: https://doi.org/10.3390/cryst10030226

[23] S.K. Ali, H. Wani, C. Upadhyay, K.S. Madhur, I. Khan, S. Gul, N. Jahan, F. Ali, S. Hussain, K. Azmi, Indones. Phys. Rev. **3** (3), 100-110 (2020). DOI: https://doi.org/10.29303/ipr.v3i3.64

[24] D. Ponnamma, J.-J. Cabibihan, M. Rajan, S.S. Pethaiah, K. Deshmukh, J.P. Gogoi, S.K. Pasha, M.B. Ahamed, J. Krishnegowda, B.N. Chandrashekar, Mater. Sci. Eng. C **98**, 1210-1240 (2019). DOI: https://doi.org/10.1016/j.msec.2019.01.081

[25] J. Loste, J.-M. Lopez-Cuesta, L. Billon, H. Garay, M. Save, Prog. Polym. Sci. **89**, 133-158 (2019). DOI: https://doi.org/10.1016/j.progpolymsci.2018.10.003